Chirality transitions in a system of active flat spinners. Supplementary Material

Miguel A. López-Castaño[1], Alejandro Márquez Seco[1], Alicia Márquez Seco[1], Álvaro Rodríguez-Rivas[2], and Francisco Vega Reyes[1,*]

[1]Departamento de Física and Instituto de Computación Científica Avanzada (ICCAEx), Universidad de Extremadura, 06071 Badajoz, Spain
[2]Department of Physical, Chemical and Natural Systems, Pablo de Olavide University, 41013, Sevilla, Spain
[*]fvega@eaphysics.xyz

ABSTRACT

Supplementary Material file with theory and additional data.

1 Theoretical expressions

We denote the single particle distribution function, at a given time t, as $f(\mathbf{r},\mathbf{v},\mathbf{w};t)$, where $\mathbf{r}$ is the particle position, $\mathbf{v}$ is the particle velocity and $\mathbf{w}$ the particle spin (angular velocity).

The marginal distribution functions, used in Figure 1 are defined as

$$f_{r,w}(v) = (1/n(r))\int \mathrm{d}\mathbf{r}\int \mathrm{d}\mathbf{v}\int \mathrm{d}\mathbf{w} f(r,\mathbf{v},\mathbf{w})\delta(|\mathbf{v}-v|)$$
$$f_{r,v}(w) = (1/n(r))\int \mathrm{d}\mathbf{r}\int \mathrm{d}\mathbf{v}\int \mathrm{d}\mathbf{w} f(r,\mathbf{v},\mathbf{w})\delta(w_z-w), \tag{1}$$

where $n(r)$ is the particle density field. The relevant fields are defined as

$$n(r) = \int \mathrm{d}\mathbf{v}\int \mathrm{d}\mathbf{w} f(r,\mathbf{v},\mathbf{w}), \quad \mathbf{u}(r) = (1/n(r))\int \mathrm{d}\mathbf{v}\int \mathrm{d}\mathbf{w}\, f(r,\mathbf{v},\mathbf{w})\mathbf{v}, \quad \mathbf{\Omega}(r) = (1/n(r))\int \mathrm{d}\mathbf{v}\int \mathrm{d}\mathbf{w}\, f(r,\mathbf{v},\mathbf{w})\mathbf{w} \tag{2}$$
$$T_t(r) = \frac{m}{2n(r)}\int \mathrm{d}\mathbf{v}\int \mathrm{d}\mathbf{w} f(r,\mathbf{v},\mathbf{w})(\mathbf{v}-\mathbf{u}(r))^2, \quad T_r(r) = \frac{I}{2n(r)}\int \mathrm{d}\mathbf{v}\int \mathrm{d}\mathbf{w} f(r,\mathbf{v},\mathbf{w})w^2, \tag{3}$$

with $w \equiv |\mathbf{w}| = |w_z|$ and m, I are particle mass and moment of inertia, respectively. We also define the spin thermal fluctuations

$$T_r^*(r) = \frac{I}{2n(r)}\int \mathrm{d}\mathbf{v}\int \mathrm{d}\mathbf{w} f(r,\mathbf{v},\mathbf{w})(\mathbf{w}-\mathbf{\Omega})^2, \tag{4}$$

The scale of thermal fluctuations for translations (T_t) and rotations (T_r^*) in our system will in general be different. For convenience, we define $\mathbf{V} = \mathbf{v}-\mathbf{u}(\mathbf{r})$, $\mathbf{W} = \mathbf{w}-\mathbf{\Omega}(\boldsymbol{r})$. Let us also define the bivariate Maxellian

$$f_{2M}(r,V,W) = (n(r)mI/(4\pi^2 T_t(r)T_r^*(r)))\mathrm{e}^{-\frac{V^2}{2T_t m}}\mathrm{e}^{-\frac{W^2}{2T_r^* I}} \equiv (n/(4\pi^2 T_t(r)T_r^*(r)))\mathrm{e}^{-V^{*2}}\mathrm{e}^{-W^{*2}}. \tag{5}$$

Henceforth, we use the notation: $A^{*j} = A^j/(2T_t/m)^{j/2} \equiv A^j/\langle V^2\rangle^{j/2}$, $B^{*j} = B/(2T_r^*/I) \equiv B^j/\langle W^2\rangle^{j/2}$ for j-th powers of translational velocities and angular velocities, respectively. We can write the distribution function as a polynomial expansion around $f_{2M}(r,V,W)$.

$$f(r,\mathbf{v},\mathbf{w}) = \frac{n(r)}{\pi^2}\left(\frac{mI}{4T_t(r)T_r^*(r)}\right)\mathrm{e}^{-V^{*2}}\mathrm{e}^{-W^{*2}}\sum_{j,k,\ell=0}^{\infty} a_{jk}^{(\ell)} L_j^{(\ell+\ell_0)}(V^{*2})L_k^{(\ell+\ell_0')}(W^{*2})(V^*W^*)^{2\ell}P_\ell(\cos\alpha) = \tag{6}$$

$$f_{2M}(r,V,W)\sum_{j,k,\ell=0}^{\infty} a_{jk}^{(\ell)} L_j^{(\ell)}(V^{*2})L_k^{(\ell)}(W^{*2})(V^{*2}W^{*2})^{\ell}P_\ell(\cos\alpha), \tag{7}$$

where ℓ_0, ℓ'_0 are constants to be chosen later, and $\cos\alpha \equiv (\mathbf{v}\times\mathbf{w})\cdot\hat{\mathbf{e}}_\varphi/|\mathbf{v}\times\mathbf{w}|$. Symbols $L_j^{(\ell)}(x)$, with ℓ being an integer, stand for the associated Laguerre polynomials of order (j,ℓ), and with $x \in [0,\infty]$. They are also commonly denoted, in the context of kinetic theory, as Sonine polynomials[1,2]. Also, P_ℓ are the Legendre polynomials. The product of Associated Laguerre and Legendre polynomials both configure the set of orthogonal polynomials $L_j^{(\ell)}(V^{*2}L_k^{(\ell)}(W^{*2})(V^*W^*)^{2p\ell}P_\ell(\cos\alpha)$ in (7). Specifically, from the orthogonality conditions of the Associated Laguerre and Legendre follows trivially

$$\int_0^\infty \mathrm{d}v \int_0^\infty \mathrm{d}w \int_{-1}^{+1} \mathrm{d}(cos\alpha)\left(L_j^{(\ell)}(V^{*2})L_k^{(\ell)}(W^{*2})P_\ell(\cos\alpha)\right)\left(L_{j'}^{(\ell')}(V^{*2})L_{k'}^{(\ell')}(W^{*2})P_{\ell'}(\cos\alpha)\right)\mathrm{e}^{-V^{*2}}\mathrm{e}^{-W^{*2}}(V^{*2}W^{*2})^\ell$$
$$= \frac{\Gamma(j+\ell+1)}{j!}\frac{\Gamma(k+\ell+1)}{k!}\frac{2}{2\ell+1}\delta_{j,j'}\delta_{k,k'}\delta_{\ell,\ell'}, \tag{8}$$

and therefore

$$\int \mathrm{d}\mathbf{v}\mathrm{d}\mathbf{w} L_1^{(\ell_0)}(V^{*2})L_0^{(\ell'_0)}(W^{*2})P_0(cos\alpha)f(r,\mathbf{v},\mathbf{w}) = \int \mathrm{d}\mathbf{v}\mathrm{d}\mathbf{w}(1+\ell_0-V^{*2})f(r,\mathbf{v},\mathbf{w}) = \left(1+\ell_0-\frac{\langle V^2\rangle}{2T_t(r)n(r)/m}\right)n(r), \tag{9}$$

where we have taken into account (3) and that $V^{*2} \equiv V^2/(2T_t/m)$.

On the other hand, from the polynomial expansion (7)

$$\int \mathrm{d}\mathbf{v}\mathrm{d}\mathbf{w} L_1^{(\ell_0)}(V^{*2})L_0^{(\ell'_0)}(W^{*2})P_0(cos\alpha)f(r,\mathbf{v},\mathbf{w}) = \frac{n(r)mI}{4\pi^2 T_t(r)T_r^*(r)}\times$$
$$\sum_{j,k,\ell=0}^\infty a_{jk}^{(\ell)}\int \mathrm{d}\mathbf{v}\mathrm{d}\mathbf{w} L_1^{(\ell')}(V^{*2}))L_j^{(\ell_0)}(V^{*2})L_0^{(\ell')}(W^{*2})L_k^{(\ell'_0)}(W^{*2})\mathrm{e}^{-V^{*2}}\mathrm{e}^{-W^{*2}}(V^*W^*)^{2\ell}P_0(\cos\alpha)P_\ell(\cos\alpha) =$$
$$n(r)\sum_{j,k,\ell=0}^\infty a_{jk}^{(\ell)}\frac{\Gamma(1+\ell_0+1)}{1!}\frac{\Gamma(0+\ell'_0+1)}{0!}\frac{2}{2\ell+1}\delta_{j,j'}\delta_{k,k'}\delta_{\ell,\ell'} = \Gamma(\ell_0+2)\Gamma(\ell'_0+1)n(r)a_{10}^{(\ell)}, \tag{10}$$

and, therefore, combining (9), (10)

$$\Gamma(\ell_0+2)\Gamma(\ell'_0+1)a_{10}^{(\ell)} = 1+\ell_0-\frac{\langle V^2\rangle}{2n(r)T_t(r)/m}. \tag{11}$$

The equation above makes evident the convenient choice $\ell_0, \ell'_0 = 0$, for which (11) yields

$$a_{10}^{(\ell)} = 1-\frac{\langle V^2\rangle}{2T_t/m} = 0, \tag{12}$$

since the definition of average translational kinetic energy T_t in (3) implies that $(m/2)\langle V^2\rangle = T_t$. Moreover, the choice $\ell_0, \ell'_0 = 0$ implies that all $a_{j,k}^{(\ell)} = 0$ except the zeroth order contribution $a_{00}^{(0)}$, if the particle distribution function is the 2D Maxwellian (i.e.,$f = f_{2M}$) thus these constants (usually called cumulants or Sonine coefficients in the context of kinetic theory) measure deviations from the Maxwellian (i.e., from the thermodynamic equilibrium state).

For this reason, we write the distribution function as

$$f(r,\mathbf{v},\mathbf{w}) = f_{2M}(r,V,W)\sum_{j,k,\ell=0}^\infty a_{jk}^{(\ell)}L_j^{(\ell)}(V^{*2})L_k^{(\ell)}(W^{*2})(V^*W^*)^{2\ell}P_\ell(\cos\alpha). \tag{13}$$

Notice that for $\ell_0, \ell'_0 = 0$ the first three associated Laguerre polynomials are $L_0^\ell(x) = 1$, $L_1^{(\ell)}(x) = 1-x$, $L_2^{(\ell)}(x) = x^2/2 - 2x+1$. On the other hand, the first two Legendre polynomials are $P_0(y) = 1$, $P_1(y) = y$. By replacing $x \to V^{*2}, W^{*2}$ and $y \to \cos\alpha$ we repeating the procedure in (10), (11) for the polynomial combinations $L_2^{(0)}(V^{*2})L_0^{(0)}(W^{*2})P_0(\cos\alpha)$,

$L_0^{(0)}(V^{*2})L_2^{(0)}(W^{*2})P_0(\cos\alpha)$, $L_1^{(0)}(V^{*2})L_1^{(0)}(W^{*2})P_0(\cos\alpha)$ and $L_0^{(1)}(V^{*2})L_0^{(1)}(W^{*2})P_1(\cos\alpha)$ we obtain, respectively, the first four cumulants

$$a_{20}^{(0)}(r) = \frac{1}{2}\frac{\langle V^4\rangle}{\langle V^2\rangle^2} - 1, \quad a_{02}^{(0)}(r) = \frac{1}{2}\frac{\langle W^4\rangle}{\langle W^2\rangle^2} - 1, \quad a_{11}^{(0)}(r) = \frac{1}{2}\left(\frac{\langle V^2W^2\rangle}{\langle V^2\rangle\langle W^2\rangle} - 1\right), \quad a_{00}^{(1)}(r) = \frac{3}{2}\frac{\langle(\mathbf{v}\times\mathbf{w})\cdot\hat{\mathbf{e}}_\varphi\rangle}{\sqrt{\langle V^2\rangle\langle W^2\rangle}}. \tag{14}$$

Notice that the expression for that would result from (13) actually is $a_{00}^{(1)} = \frac{3}{2}\left\langle V^{*2}W^{*2}\frac{(\mathbf{v}\times\mathbf{w})\cdot\hat{\mathbf{e}}_\phi}{|\mathbf{v}\times\mathbf{w}|}\right\rangle = \frac{3}{2}\left\langle V^*W^*(\mathbf{v}^*\times\mathbf{w}^*)\cdot\hat{\mathbf{e}}_\phi\right\rangle$. However, we choose a rescaled version of $a_{00}^{(1)}$ without the factor V^*W^*, so that represents a closer analog of the bend coefficient in liquid crystals[3].

2 Additional Information

In this work we have recorded a total 120 movies covering a wide range of densities, going from $\phi = 0.03$ to $\phi = 0.70$. We could not represent all our results in the main text; therefore, here we include additional figures, complementary movies and experimental data.

- **Additional figures:** The first supplementary figure is analog to Figure 1 in the main text, covering the $\phi = 0.55$ density case, in this figure one can see that the bimodal behavior of the spin distribution function is stronger than in the lower density case (shown in the main text). Also, from panels **c-j** we now see that particle cover the entire area of the system. The second supplementary figure includes data for the cumulants defined in Eq. 2 (main text) that are not covered by Figure 4 in the article.
- **Supplementary movies:** We included two additional videos in order to help the reader understand the most relevant results. In supplementary video 1, we show three configurations with constant density but an increasing thermalization level ($T_t = \{0.63,\ 1.16,\ 2.65\}\ m_p(\sigma/\mathrm{s})^2$), this movie illustrate the chirality reversal caused by interaction with the system boundaries, we display the trajectories of three representative particles for each case. Supplementary video 2 in turn displays the temporal evolution of the vorticity field for a sample experiment, there we show a situation of complex chirality with several vortexes of opposite directions, these vortexes evolve with time.
- **Experimental data:** The experimental data used for generating all figures are included in a repository[4]. These files contain the full trajectories of all particles in a given experiment and the angular velocity of the disks. Additional data and the processing code is also available upon request to the authors.

References

1. Sonine, N. Recherches sur les fonctions cylindriques et le développement des fonctions continues en série. *Math Ann.* **16**, 1 (1880).
2. van Noije, T. P. C. & Ernst, M. H. Velocity distributions in homogeneous granular fluids: the free and the heated case. *Granul. Matter* **1**, 57–64 (1998).
3. Chaikin, P. M. & Lubensky, T. C. *Principles of Condensed Matter Physics* (Cambridge University Press, Cambridge, UK, 2000).
4. Supplementary file with information on experimental methods, experiments movie clips, and additional figures in `http://doi.org/10.5281/zenodo.4740831`.

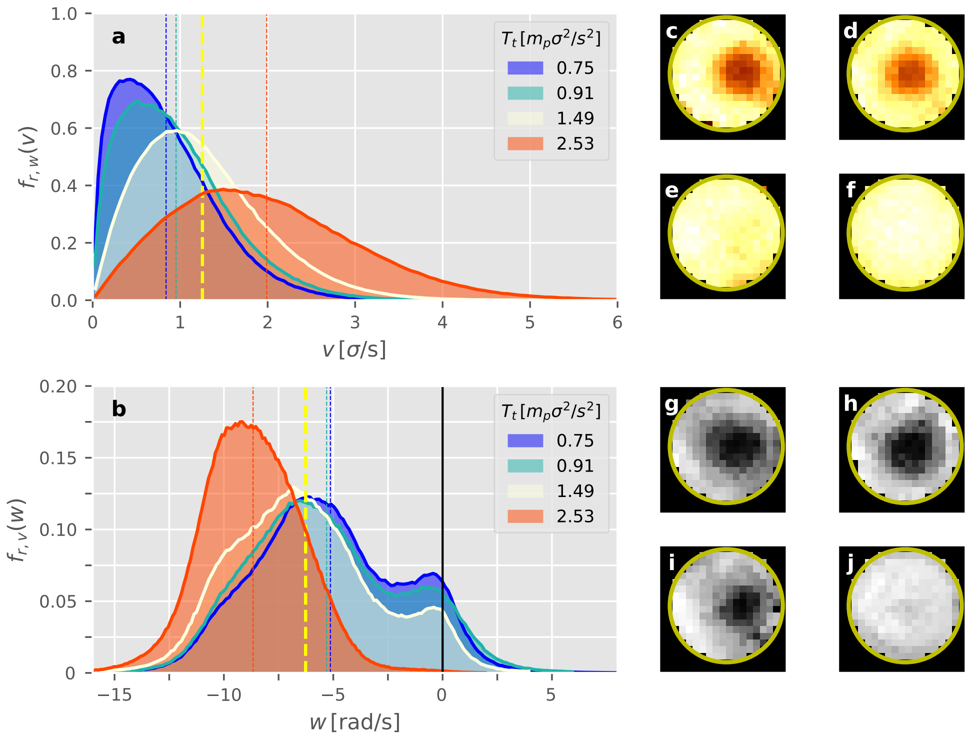

Additional Figure 1. **a** Traslational particle velocity distribution (v), $f_{r,w}(v)$ for a system with $\phi = 0.55$; **b** particle spin distribution (w), $f_{r,v}(w)$. **c-f** Reduced particle speed fluctuations $U^*(x,y) \equiv v_{\mathrm{th}}(x,y)/V_0$. **g-j** Reduced average spin $\Omega^*(x,y) \equiv \langle w(x,y) \rangle / w_0$. In both $U^*(x,y)$ and $\Omega^*(x,y)$ color maps, brighter is higher and darker is lower; and black stands for $U^*(x,y), \Omega^*(x,y) = 0$ and white for $U^*(x,y), \Omega^*(x,y) = 1$. T_t is in units of $m_p\sigma^2/\mathrm{s}^2$. The system boundary is marked with a thick yellow line.

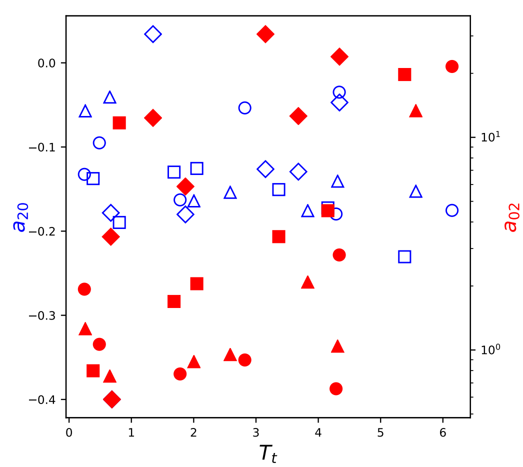

Additional Figure 2. In this figure we plot the cumulants $a_{20}^{(0)}$ (blue, Y axis at the left), $a_{02}^{(0)}$ (red, Y axis at the right in logarithmic scale) for the spin and velocity distributions. Each point represents the value for a single experiment, we show that, besides the systems being clearly not Maxwellian (values far from zero), there is no clear trend in their value as we change the thermalization level.